

Gene Knockout and Metabolome Analysis of Carnitine/Organic Cation Transporter OCTN1

メタデータ	言語: eng 出版者: 公開日: 2017-10-04 キーワード (Ja): キーワード (En): 作成者: メールアドレス: 所属:
URL	http://hdl.handle.net/2297/23502

Gene Knockout and Metabolome Analysis of Carnitine/Organic Cation Transporter OCTN1

Yukio Kato,¹ Yoshiyuki Kubo,¹ Daisuke Iwata,¹ Sayaka Kato,¹ Tomohisa Sudo,¹ Tomoko Sugiura,¹
Takashi Kagaya,² Tomohiko Wakayama,³ Akiyoshi Hirayama,⁴ Masahiro Sugimoto,⁴ Kazushi
Sugihara,⁵ Shuichi Kaneko,² Tomoyoshi Soga,⁴ Masahide Asano,⁵ Masaru Tomita,⁴ Toshiyuki Matsui,
⁶ Morimasa Wada,⁷ and Akira Tsuji^{1,8}

¹Division of Pharmaceutical Sciences, Graduate School of Natural Science and Technology, Kanazawa
University, Kanazawa 920-1192, Japan, ²Department of Gastroenterology, Kanazawa University
Hospital, Kanazawa 920-0934, Japan, ³Department of Histology and Embryology, Graduate School of
Medical Science, Kanazawa University, Kanazawa 920-0934, Japan, ⁴Institute for Advanced
Biosciences, Keio University, Yamagata 997-0035, Japan, ⁵Division of Transgenic Animal Science,
Advanced Science Research Center, Kanazawa University, Kanazawa 920-0934, Japan, ⁶Department of
Gastroenterology, Fukuoka University Chikushi Hospital, Fukuoka 818-8502, Japan, ⁷Division of
Molecular Biology, Faculty of Pharmaceutical Sciences, Nagasaki International University, Nagasaki
859-3298, Japan, and ⁸To whom correspondence should be addressed. (e-mail:

tsuji@kenroku.kanazawa-u.ac.jp)

Running Head: Gene Knockout and Metabolome Analysis of OCTN1

Correspondence: Prof. Akira Tsuji, Ph.D., Division of Pharmaceutical Sciences, Graduate School of Natural Science and Technology, Kanazawa University, Kakuma-machi, Kanazawa 920-1192, Japan.

Phone: (81)76-264-5085; Fax: (81)76-234-4010; E-mail: tsuji@kenroku.kanazawa-u.ac.jp

Abstract

Purpose: Solute carrier, OCTN1 (SLC22A4) is an orphan transporter, the physiologically important substrate of which is still unidentified. The aim of the present study was to examine physiological roles of OCTN1.

Methods: We first constructed *octn1* gene knockout (*octn1*^{-/-}) mice. Metabolome analysis was then performed to identify substrates *in vivo*. The possible association of the substrate identified with diseased conditions was further examined.

Results: The metabolome analysis of blood and several organs indicated complete deficiency of a naturally occurring potent antioxidant ergothioneine in *octn1*^{-/-} mice among 112 metabolites examined. Pharmacokinetic analyses after oral administration revealed the highest distribution to small intestines and extensive renal reabsorption of [³H]ergothioneine, both of which were much reduced in *octn1*^{-/-} mice. The *octn1*^{-/-} mice exhibited greater susceptibility to intestinal inflammation under the ischemia and reperfusion model. The blood ergothioneine concentration was also much reduced in Japanese patients with Crohn's disease, compared with healthy volunteers and patients with another inflammatory bowel disease, ulcerative colitis.

Conclusions: These results indicate that OCTN1 plays a pivotal role for maintenance of systemic and intestinal exposure of ergothioneine which could be important for protective effect against intestinal tissue injuries, providing a possible diagnostic tool to distinguish the inflammatory bowel diseases.

Key Words: Transporter, OCTN1, Crohn's Disease, Metabolome Analysis, Gene Knockout

Introduction

Carnitine/organic cation transporter OCTN1 (SLC22A4) was originally identified in our laboratory as a multispecific transporter which preferentially recognizes organic cations and, to a lesser extent, carnitine, which is essential for β -oxidation of fatty acids in mitochondria, as substrates (1,2). In addition, Gründemann *et al* have previously reported that ergothioneine is also the good substrate for OCTN1 *in vitro*, by utilizing cell biological and metabolomics approaches (3). Despite the previous identification of various substrates for OCTN1 in *in vitro* experimental systems, biologically important substrates for OCTN1 *in vivo* have not yet been clarified. OCTN2 (SLC22A5) is another member of the OCTN family and is much more carnitine-selective (4,5). A physiologically pivotal role of OCTN2 in reabsorption of carnitine in proximal tubules has already been identified: a missense mutation in the *octn2* gene of a naturally occurring mutant, juvenile visceral steatosis (*jvs*) mouse, or in the *OCTN2* gene of humans leads to systemic carnitine deficiency (6).

Both *OCTN1* and *OCTN2* genes are located on cytokine cluster region in chromosome 5q, which is possibly associated with various inflammatory diseases. *OCTN1* gene was actually reported to be associated with rheumatoid arthritis (7), whereas both *OCTN1* and *OCTN2* genes have been proposed to contribute directly to susceptibility to Crohn's disease (CD) in European people (8). However, the reported mutations in these genes (C1672T and G-207C, respectively) were absent or not associated

with CD in Japanese patients (9), supporting the existence of ethnic difference in genetic variants causative of CD. In addition, the variants in these two genes appeared not to be causative even in European populations according to a recent analysis of more than a thousand pairs (10). Thus, the precise locus directly linked to CD susceptibility has not yet been elucidated, probably because of the limitations of a purely genetic approach.

Considering the association of the *OCTN2* gene with CD (8), experimental animals with mutation of the *octn2* gene would be useful tools to explore the pathogenesis of CD. This idea is supported by recent findings of spontaneous development of intestinal atrophy and inflammation in *jvs* mice, demonstrating an obligatory role of OCTN2 in the maintenance of normal intestinal morphology (11). On the other hand, little is known about the physiological role of OCTN1, mainly because appropriate gene-deficient animals are not available. In the present study, we first developed *octn1* gene knockout (*octn1^{-/-}*) mice with the aim of employing them to examine the biological roles and possible association of OCTN1 with any diseased conditions. The metabolome analysis using capillary electrophoresis time-of-flight mass spectrometry (CE-TOFMS) of blood and several organs indicated complete deficiency in *octn1^{-/-}* mice of a naturally occurring potent antioxidant ergothioneine which was found to be highly accumulated in small intestine after oral administration. The greater susceptibility to intestinal

inflammation in the *octn1*^{-/-} mice and the lower blood levels of ergothioneine in Japanese CD patients may suggest possible linkage between this antioxidant and small intestinal diseases.

Materials and Methods

Construction of *octn1* Gene Knockout (*octn1*^{-/-}) Mice.

The *octn1*^{-/-} mice were generated according to the method previously reported (12). PCR was first performed with genomic DNA derived from E14-1 ES cells in order to isolate the homologous regions of *octn1* gene. The targeting vector consisted of 8.5 kb of the 3' homologous region, 1.2 kb of the 5' homologous region of *octn1* gene, the neomycin resistance (Neo^r) gene cassette driven under the phosphoglycerate kinase I promoter (13) and subunit A of the diphtheria toxin (DT-A) gene cassette driven under the MC1 promoter (14). With this targeting vector, exon 1 (including the start codon) should be deleted (Supplementary Figure 1). The vector construction and purification was performed by means of *E. coli* DH5 α . The linearized targeting vector (20 μ g) was then electroporated into ES cells, and recombinants were selected with 180 mg/mL of active form G418 (Gibco/BRL) for 7 - 10 days. More than 500 clones of embryonic stem cells were screened by genomic PCR. Three of them were subjected to Southern blot analysis, and two clones (1B5 and 3B3) were selected to generate *octn1*^{-/-} mice (Supplementary Figure 1B). Chimeric mice were generated by the aggregation method. Chimeras were mated with C57BL/6J females, and homozygous mutant mice were generated by crossing of the heterozygotes. Mice were given normal commercial diet, PicoLab Rodent Diet 20 (PMI Nutrition International, St. Louis, MO), and water ad libitum. They were kept in an environmentally controlled

clean room at the Institute of Experimental Animals, Advanced Science Research Center, Kanazawa University.

Genotypes in mice were determined by a PCR method using genomic DNA prepared from mouse ear. The forward primer (5'-catttcagaagtaagaaaccctgag-3') was localized outside the targeting vector, whereas the reverse primer outside exon 1 (5'-gaaagtggggcctcgacatag-3') or that at the end of the PGKneobpA cassette (5'-ctatggcttctgaggcggaagaacc-3') was used to detect wild-type and mutant locus, respectively (Supplementary Figure 1A). PCR was carried out for 40 cycles at 94°C for 30 sec, 64°C for 30 sec and 72°C for 2.5 min using a Platinum PCR SuperMix (Invitrogen). Deletion of the *octn1* gene and loss of expression of the gene product in kidney membrane fraction of *octn1*^{-/-} mice were confirmed (Supplementary Figure 1C and D). All the animal experiments were performed according to the Guidelines for the Care and Use of Laboratory Animals in Kanazawa University.

Southern blot analysis.

Southern blot was performed as previously described (15). Genomic DNA prepared from mouse liver was digested with *Xba* I, electrophoresed through a 0.8% agarose gel, and transferred to Hybond-N+ (GE Healthcare). Hybridization was carried out using ³²P-labeled DNA probes made by Megaprime DNA Labelling System (GE Healthcare).

Western blot analysis.

Western blot was performed as previously described (15). The membrane fraction prepared from mouse kidneys were separated by 12% SDS-polyacrylamide gel, followed by the transfer of the proteins to polyvinylidene difluoride membrane (Immobilon, Millipore). The membrane was incubated with polyclonal anti-peptide antibodies against the carboxyl terminus of mouse OCTN1 for 2 hr, and then incubated with secondary antibody (donkey anti-rabbit IgG, horseradish peroxidase-linked whole antibody, GE Healthcare). The proteins were detected by means of the enhanced chemiluminescence detection method using the ECL Plus Western-blotting detection system (GE Healthcare).

Differential metabolomics.

The wild-type and *octn1*^{-/-} mice were fasted overnight with free access to water and then anesthetized with pentobarbital (60 mg/kg), followed by collection of urine from a bladder cannula for 30 min. Blood and tissues were then obtained, and metabolites were extracted and subjected to CE-TOFMS analysis as described previously for detection of cationic and anionic metabolites, and nucleotides (16,17).

Analysis of ergothioneine by means of HPLC.

All the tissue samples were weighed, and portions were homogenized with two volumes of distilled water. The homogenized tissues, urine, plasma and blood were deproteinized with acetonitrile and subjected to HPLC after centrifugation. The HPLC system incorporated a model PU-2080 pump and a model UV-2075 monitor (Jasco) with a 250 x 4.6 mm i.d. Atlantis HILIC silica column (Waters). The mobile phase was 0.1 M ammonium formate and methanol at a ratio of 95:5. The flow rate was 1 mL/min. The wavelength for UV detection was 268 nm. Cephaloridine was used as the internal standard.

Pharmacokinetic study in mice.

Male mice (8 weeks old) were fasted overnight with access to water, and anesthetized by intraperitoneal injection of pentobarbital. After oral administration of [³H]ergothioneine (Moravek Biochemicals) at 330 µg/kg, each mouse was kept in a metabolic cage during the experiment. Blood samples were collected from the tail vein using heparinized capillary tubes at 1 h, and 1, 2, 3, 5, 7, 10 and 14 days under anesthesia. Urine samples were collected using a metabolic cage. Plasma, blood and urine samples were mixed with scintillation fluid (Clearsol, Nakarai Tesque) for quantitation. At 14 days, tissues were excised, rinsed with ice-cold saline, blotted to dryness and weighed. Tissue samples

(0.05-0.2 g) were dissolved in 1 mL of Soluene-350 (Packard), mixed with scintillation fluid, and neutralized with 5 M HCl, followed by determination of the associated radioactivity.

Intestinal ischemia and reperfusion injury.

Male mice (10-12 weeks old) were fasted for 18-20 hr with free access to water and anesthetized by intraperitoneal injection of pentobarbital. A midline laparotomy was performed, and the superior mesenteric artery was occluded with an arterial microclamp. Intestinal ischemia was confirmed by pulselessness of the mesentery and paleness of the intestine. After 60 min the clamp was removed, and the mice were sutured. Intestinal tissue sections were deparaffinized, rehydrated and stained with hematoxylin and eosin. Differences in survival of wild-type and *octn1*^{-/-} mice were determined by means of the log-rank test. Statistical analysis was performed using GraphPad Prism version 4.0 (GraphPad Software San Diego).

Transport studies in renal brush border membrane vesicles

The brush border membrane vesicles were prepared essentially as previously described with a little modification (18). Transport studies were performed by rapid filtration technique at 25°C.

Blood sampling in humans.

Unrelated Japanese adult patients with CD (n = 25, 14 ~ 47 years old, 18 male and 7 female) and ulcerative colitis (UC, n = 16, 18 ~ 70 years old, 8 male and 8 female) were enrolled from Kanazawa University Hospital. Unrelated Japanese adult healthy volunteers (n = 31, 21 ~ 36 years old, 22 male and 9 female) were recruited from Kanazawa University Hospital and the Faculty of Pharmaceutical Sciences, Kanazawa University. Informed consent was obtained from all the subjects. The study protocol was approved by the ethics committee of Kanazawa University Graduate School of Medical Science (Kanazawa, Japan) and the study was carried out in accordance with the Declaration of Helsinki. Blood samples (5 ~ 10 mL) were drawn from the brachial vein of the subjects. Statistical analysis was performed by means of one-way ANOVA followed by Dannett's multiple comparison test.

Genotyping in human samples.

Blood samples were obtained from Japanese adult patients (N = 256) with CD in Kanazawa University Hospital, Kyushu University Hospital and Fukuoka University Hospital. DNA was isolated using the QIAamp DNA Blood Mini Kit (QIAGEN, Tokyo, Japan). The DNA sequence was analyzed by sequence-specific PCR using the primers shown in Supplementary Table 1. The genomic sequencing

was performed for all the exons of *OCTN1* and *OCTN2*. Since several introns can also be sequenced by the primers used in the present study, allelic frequency of such introns was also analyzed. The SNP at the 5'-UTR region of *OCTN2* (G-207C) was previously reported to be associated with CD in Caucasians (8), and was also analyzed in the present study. Exon 1 of *OCTN1*, and the 5'-UTR and exon 1 of *OCTN2* were amplified in a total volume of 25 μ l, with 5 ng of genomic DNA, 10 μ M of each amplification primer, 2.5 mM of each dNTP, 2 x GC rich buffer I and 1.25 units of LA Taq DNA polymerase (TaKaRa). The PCR reaction was initial denaturation at 94 °C for 2 min, followed by 35 cycles of denaturation at 94 °C for 30 s, annealing for 30 s and extension at 72 °C, and a final extension at 72 °C for 7 min. The annealing temperature and extension time are shown in Supplementary Table 1. Other regions were amplified in a total volume of 25 μ L, with 5 ng of genomic DNA, 10 μ M of each amplification primer, 2.5 mM of each dNTP, 5 x Expand High Fidelity Reaction buffer without 7.5 mM MgCl₂ and 2.5 units of Expand High Fidelity Enzyme Blend (Roche). All samples were sequenced using a BigDye Terminator v3.1 Cycle Sequencing Kit (ABI PRISM). The sequence reaction was initiated by denaturation at 96 °C for 2 min, followed by 35 cycles of 96 °C for 10 s, 50 °C for 5 sec and 60 °C for 1 min, and a final extension at 60 °C for 7 min. All samples were confirmed by sequencing on an ABI 310 DNA sequencer (Applied Biosystems). The study protocol was approved by the ethical committees of Kanazawa University, Kyushu University and Fukuoka University

Results

Metabolome analysis revealed complete loss of ergothioneine in the *octn1*^{-/-} mice.

Targeted disruption of the *octn1* gene was first performed by homologous recombination. The *octn1*^{-/-} mice thus obtained were born at the expected Mendelian ratio (Supplementary Figure 1E), developed normally and did not display any gross phenotypic abnormalities. Most of the biochemical parameters of sera examined exhibited minimal difference between wild-type and *octn1*^{-/-} mice, and some parameters exhibited minor, but significant difference only in female mice (Supplementary Table 2). To identify any possible phenotypes observed in the *octn1*^{-/-} mice, we then applied a metabolome differential display method based on capillary electrophoresis time-of-flight mass spectrometry (CE-TOFMS) (16) to compare the metabolites of wild-type and *octn1*^{-/-} mice. Only ergothioneine was found to be completely absent in erythrocytes of *octn1*^{-/-} mice (Supplementary Figure 2). In this analysis, we quantitatively measured 112 metabolites by means of CE-TOFMS (16,17) and confirmed the loss of ergothioneine in heart, liver, small intestine, kidney and erythrocytes of *octn1*^{-/-} mice (Figure 1). Ergothioneine level was further examined in various tissues, plasma and urine by means of HPLC, confirming complete loss of ergothioneine in all the tissue samples examined and plasma of *octn1*^{-/-} mice (Table I).

Ergothioneine is a substrate of mouse OCTN1

When mouse OCTN1 or OCTN2 was heterologously transfected in HEK293 cells, only OCTN1, but not OCTN2 efficiently transports ergothioneine as a substrate (Figure 2A), as previously reported for human and rat OCTN1 (3,19). The uptake of [³H]ergothioneine by mouse OCTN1 was saturable with K_m and V_{max} values of 4.68 μ M and 532 pmol/min/mg protein, respectively (Figure 2B) and reduced by the replacement of Na⁺ in the medium (Figure 2C).

Intestinal absorption, distribution to small intestine and renal reabsorption of ergothioneine

In general, ergothioneine is known as an extremely stable antioxidant which can directly scavenge reactive oxygen species, thereby protecting tissues against oxidative stress (20,21). Due to the minimal endogenous biosynthesis, the major source of ergothioneine for animals and plants is fungi and mycobacteria in soil (21). Because quite limited information is available on details in biodistribution kinetics of ergothioneine in the body, we next examined the absorption and disposition of [³H]ergothioneine after oral administration. The plasma concentration of [³H]ergothioneine transiently increased and then gradually decreased in *octn1*^{-/-} mice, whereas that in wild-type mice was maintained for at least two weeks after oral administration (Figure 3A). This result was compatible with the much higher accumulation of [³H]ergothioneine also in erythrocytes of wild-type mice (Figure 3B). The

disappearance of [³H]ergothioneine in *octn1*^{-/-} mice could be due to the higher urinary excretion in *octn1*^{-/-} mice, compared with wild-type mice (Figure 3C). Overshoot uptake of [³H]ergothioneine was observed in renal brush-border membrane vesicles prepared from wild-type mice, but not in *octn1*^{-/-} mice (Supplementary Figure 3). This suggests that ergothioneine is reabsorbed by OCTN1 in wild-type mice, but not in *octn1*^{-/-} mice if we consider that OCTN1 is localized on brush-border membranes of proximal tubules (22).

The tissue distribution of [³H]ergothioneine after oral administration was then analyzed in both strains (Figure 4). The highest concentration of [³H]ergothioneine was observed in upper and middle parts of small intestine at 4 hr after oral administration in wild-type mice (Figure 4A). However, such accumulation in small intestine cannot be observed in *octn1*^{-/-} mice (Figure 4A). The distribution of [³H]ergothioneine to small intestine and other tissues was observed even at 14 days after oral administration in wild-type mice, but the distributed amount was much smaller in *octn1*^{-/-} mice (Figure 4B).

The *octn1*^{-/-} mice showed a lower tolerance to intestinal oxidative stress.

Ergothioneine concentration in the small intestine was approximately 0.1 mM (~20 µg/mL, Table I). At such a concentration, ergothioneine behaves as a powerful chemical scavenger of a number

of oxidizing species (23). In addition, ergothioneine was found to be highly accumulated in small intestine (Figure 4), and exogenous administration of ergothioneine was reported to ameliorate oxidative stress in various tissues, including small intestine (24). These data led us to examine whether or not *octn1*^{-/-} mice were more sensitive to small intestinal injury. For this purpose, ischemia and reperfusion were performed to generate a small-intestinal inflammatory model in mice (Figure 5). After the reperfusion, lethality was significantly higher in the *octn1*^{-/-} mice than in wild-type mice (Figure 5A). This was consistent with the more obvious loss of villus structures in small intestine of *octn1*^{-/-} mice (Figure 5B).

Decreased blood levels of ergothioneine in CD patients.

The apparently greater susceptibility of *octn1*^{-/-} mice to intestinal inflammation (Figure 5) further led us to examine a possible association of ergothioneine and inflammatory bowel disease in humans as well. As shown in the Table I, the blood samples in mice showed 16.5 µg/mL of ergothioneine, whereas the plasma ergothioneine concentration was much lower and close to the detection limit of HPLC, suggesting that the blood samples would be more useful for the comparison of the ergothioneine level between healthy volunteers and patients. Therefore, the ergothioneine concentration in blood of CD and UC patients was next examined by means of HPLC. As a result, CD patients exhibited much lower

ergothioneine concentration in blood than healthy volunteers or patients with UC (Figure 6). Among the CD patients examined in the present study, no remarkable difference in the blood ergothioneine concentration was observed between patients with and without food restriction.

Genotyping of patients with CD.

To examine a direct linkage between CD and the *OCTN1* gene in the patients examined in the present study, we sequenced all the exon regions of the *OCTN1* and *OCTN2* genes, determined the allelic frequency in CD patients for SNPs reported in the NCBI database, and then compared the results with those in healthy volunteers. The mutations reported to be associated with CD patients in Caucasians (C1672T/L503F in *OCTN1* and G-207C in *OCTN2*) (8) were completely absent in Japanese CD patients examined in the present study (Supplementary Table 3). Furthermore, no other allelic frequencies exhibited a clear difference between CD patients and healthy volunteers (Supplementary Table 3).

Discussion

In the present study, *octn1*^{-/-} mice were constructed to identify the *in vivo* substrates of OCTN1 with an aim to understand physiological roles of this transporter. Ergothioneine was identified as a physiological substrate of OCTN1 in the metabolome analysis (Figure 1). Ergothioneine was previously identified as a substrate of OCTN1 in gene transfectant systems *in vitro* (3) and, therefore, was examined similarly to other over 100 compounds in the metabolome analysis. Ergothioneine has the potent antioxidant property, and the source of ergothioneine in human and animals is solely food intake due to the minimal biosynthesis (20,21). Although the mice were given normal diets without any modification in the present study, ergothioneine was detected in their tissues. It would be possible that the normal diets contained considerable amount of ergothioneine because of food chain resultant and/or contamination. The highest accumulation of ergothioneine in small intestine after oral administration (Figure 4) implies that ergothioneine may protect against oxidative stress in this tissue. The slightly, but significantly lower tolerance to intestinal oxidative stress in *octn1*^{-/-} mice (Figure 5) supports such anti-oxidant activity exerted by ergothioneine and further led us to examine the linkage between ergothioneine and CD patients (Figure 6). The diagnosis of CD is empirically based on endoscopic, radiologic and histological criteria (25). On the other hand, the present finding proposes ergothioneine as a quantitative diagnostic marker to distinguish CD from healthy subjects and UC (Figure 6). It may be

noteworthy that ergothioneine level in blood of UC patients is not so far away from that in healthy volunteers (Figure 6), indicating specificity of the blood ergothioneine level between the two inflammatory bowel diseases. As far as our knowledge, there has been no report indicating such quantitative markers which are closely relevant to CD and can be easily determined in patients. Thus, combination of gene knockout and metabolome analysis has finally revealed the basis for a diagnostic tool to distinguish CD from UC and healthy condition.

The present study has also proposed a close interrelationship between OCTN1 and ergothioneine. Ergothioneine has unique feature in its pharmacokinetics: Plasma and blood concentration of ergothioneine is maintained at least for 14 days in wild-type mice after a single oral administration (Figure 3A and B). This is probably because of large tissue distribution, tissue-to-plasma concentration ratio being more than 10 in small intestines, liver and kidney (Figure 4A), but small urinary excretion of ergothioneine, the amount excreted for 14 days after oral administration being at most 10% of dose in wild-type mice (Figure 3C). On the other hand, the plasma and blood concentration of ergothioneine transiently increased and then gradually decreased in *octn1*^{-/-} mice after oral administration (Figure 3A and B) due to much lower tissue distribution (Figure 4) and much higher urinary excretion (Figure 3C). The transient increase in plasma and blood concentration of ergothioneine in *octn1*^{-/-} mice, which appeared to be absent in wild-type mice (Figure 3A and 3B) could be explained by the remarkable

difference in the distribution of ergothioneine to the liver (Figure 4A): The K_p value in the liver exhibited approximately 200 times difference between wild-type and *octn1*^{-/-} mice (Figure 4A). This may support the hypothesis that the liver plays a first-pass elimination organ in wild-type mice, but not in *octn1*^{-/-} mice, although this hypothesis should be verified by the further analyses. The higher urinary excretion of ergothioneine in *octn1*^{-/-} mice would be due to reabsorption of ergothioneine by OCTN1 if we consider that OCTN1 is localized on brush-border membranes of proximal tubules (22), can transport ergothioneine (Figure 2) and is involved in influx of ergothioneine in renal brush-border membrane vesicles (Supplemental Figure 3). Both ergothioneine level (Table I) and tissue distribution of [³H]ergothioneine exogenously administered (Fig. 4) were almost completely reduced in *octn1*^{-/-} mice, and this was compatible with ubiquitous expression of OCTN1 in all the tissues examined (1). Thus, OCTN1 is involved in both tissue distribution and renal reabsorption of ergothioneine, thereby contributing to maintain steady-state ergothioneine level in the body.

It may be noteworthy that the wild-type mice showed distinct kinetics in the ergothioneine concentration between the plasma and blood: Ergothioneine level in blood increased slowly and reached the plateau at 6 days whereas plasma ergothioneine level was high at 1-3 days (Figure 3A and B). It was suggested that OCTN1 is highly expressed in glycophorin A-positive erythroid cells and possibly associated with erythroid-lineage cells at the transition stage from immature erythroid cells to peripheral

mature erythrocytes (26). Combined with the present results, it can be speculated that ergothioneine is taken up to the hematopoietic cells during their differentiation stage. The slow increase in the ergothioneine level in the blood (Figure 3B) could reflect the gradual increase in the number of matured blood cells containing [³H]ergothioneine.

In addition to the close interrelationship with OCTN1, ergothioneine seems to be relevant to a certain intestinal inflammatory status. This hypothesis was supported by the lower ergothioneine level in CD patients than healthy volunteers (Figure 6) and slightly lower tolerance to intestinal oxidative stress in *octn1*^{-/-} mice (Figure 5) in which ergothioneine level was under the detection limit (Table I). Exogenous administration of ergothioneine was reported to ameliorate oxidative stress in various tissues, including small intestine (24). Therefore, the effect of ergothioneine treatment on clinical symptoms of CD patients needs to be examined to clarify whether ergothioneine has a potential ameliorating effect on the intestinal inflammation. The pharmacokinetic analysis in the present study indicated that ergothioneine is orally absorbed even in *octn1*^{-/-} mice (Figure 3A and B), suggesting that ergothioneine exogenously administered could be exposed inside the small intestinal epithelium even when OCTN1 is functionally defective. While ergothioneine is generally thought to work as antioxidant in the body, its actual function *in vivo* has been questioned, indicating the possibility that ergothioneine has other unknown function directly related to CD. However, identification of the biological activities of

ergothioneine has been hindered by the absence of experimental animals deficient in ergothioneine. Because the present study has revealed minimal presence of ergothioneine in *octn1*^{-/-} mice, but much higher concentration (μM or mM level) of ergothioneine in wild-type mice (Table I), this *octn1*^{-/-} mice may be a suitable tool to demonstrate diverse activities of ergothioneine *in vivo*.

In present study, the contribution of other transporter(s) was also implied to the membrane permeation of ergothioneine. For example, ergothioneine was substantially taken up by the mock cells without transfection of *OCTN1* gene (Figure 2B), and *octn1*^{-/-} mice showed a transient increase in the plasma and blood level of ergothioneine after oral administration (Figure 3A and B). In addition, significant difference was observed in ergothioneine level between CD patients and other groups (Figure 6), but the difference was not so obvious, compared with that observed between wild-type and *octn1*^{-/-} mice (Table I). Therefore, it is possible that other transporter(s) than OCTN1 may contribute to ergothioneine transport in the body. Further studies will be needed for its molecular identification.

Gene knockout mice has been widely applied to analyze the roles of transporters, but often exhibits minimal phenotype in the knockout mice possibly due to the compensation by other transporter gene products *in vivo* and/or functional redundancy provoked by homologous transporters with overlapped substrate specificity (27,28). This may be also true for OCTN1, if we consider minimal phenotype found in *octn1*^{-/-} mice at least in normal breeding condition (see Results). Thus, application of

the metabolomics approach would be a powerful tool to identify any phenotypic difference between wild-type and the knockout mice. Metabolome analysis has been recently established to simultaneously measure whole metabolite profiles in the body, and application of this technology to whole organs of the gene knockout animals may identify physiologically important substrates, providing a clue to understand any physiological relevance of the transporters.

The possible association between CD and OCTN1 was not fully demonstrated in the present study. Association between *OCTN1* gene and CD had been controversial, and this could be compatible with the present finding that the mutations reported to be associated with CD patients in Caucasians were completely absent in Japanese CD patients (Supplementary Table 3), and that no allelic frequencies exhibited a clear difference between CD patients and healthy volunteers (Supplementary Table 3). However, steady-state ergothioneine level appears to be governed by OCTN1 according to the present findings (Table I). In addition, since ergothioneine is minimally biosynthesized or metabolized in animals (20,21,29,30), transporter(s) involved in its absorption and disposition would be likely to regulate the steady-state level of ergothioneine. Therefore, it is necessary to directly examine the function of OCTN1 in CD patients to clarify the possible relation between the lower ergothioneine level in CD patients (Figure 6) and OCTN1 activity in those patients.

In conclusion, combination of two biotechnological tools, gene knockout and metabolome analysis, has revealed pivotal role of OCTN1 in ergothioneine homeostasis which could be related to intestinal inflammations, providing the basis for a diagnostic tool for CD in humans.

Abbreviations

CD, Crohn's disease; UC, ulcerative colitis; OCTN, Organic carnitine/organic cation transporter;

CE-TOFMS, capillary electrophoresis time-of-flight mass spectrometry

Acknowledgements

We thank Lica Ishida, Kazuhiro Suzuki and Ryutaro Matsuhashi for technical assistance in Kanazawa University. We also thank Maki Sugawara and Naoko Toki for technical assistance in Keio University. We thank Prof. Shoichi Iseki in Kanazawa University for fruitful discussion. This study was supported in part by a Grant-in-Aid for Scientific Research provided by the Ministry of Education, Science and Culture of Japan, and a grant from the Mochida Memorial Foundation (Tokyo, Japan) for Medical and Pharmaceutical Research.

References

1. Tamai I, Yabuuchi H, Nezu J, Sai Y, Oku A, Shimane M, et al. Cloning and characterization of a novel human pH-dependent organic cation transporter, OCTN1. *FEBS Lett.* 1997;419:107-11.
2. Yabuuchi H, Tamai I, Nezu J, Sakamoto K, Oku A, Shimane M, et al. Novel membrane transporter OCTN1 mediates multispecific, bidirectional, and pH-dependent transport of organic cations. *J Pharmacol Exp Ther.* 1999;289: 768-73.
3. Gründemann D, Harlfinger S, Golz S, Geerts A, Lazar A, Berkels R, et al. Discovery of the ergothioneine transporter. *Proc Natl Acad Sci USA.* 2005;102:5256-61.
4. Tamai I, Ohashi R, Nezu J, Yabuuchi H, Oku A, Shimane M, et al. Molecular and functional identification of sodium ion-dependent, high affinity human carnitine transporter OCTN2. *J Biol Chem.* 1998;273:20378-82.
5. Wu X, Prasad PD, Leibach FH, Ganapathy V. cDNA sequence, transport function and genomic organization of human OCTN2, a new member of the organic cation transporter family. *Biochem Biophys Res Commun.* 1998;246:589-95.
6. Nezu J, Tamai I, Oku A, Ohashi R, Yabuuchi H, Hashimoto N, et al. Primary systemic carnitine deficiency is caused by mutations in a gene encoding sodium ion-dependent carnitine transporter. *Nat Genet.* 1999;21:91-4.

7. Tokuhiro S, Yamada R, Chang X, Suzuki A, Kochi Y, Sawada T, Suzuki M, Nagasaki M, Ohtsuki M, Ono M, Furukawa H, Nagashima M, Yoshino S, Mabuchi A, Sekine A, Saito S, Takahashi A, Tsunoda T, Nakamura Y, Yamamoto K. An intronic SNP in a RUNX1 binding site of *SLC22A4*, encoding an organic cation transporter, is associated with rheumatoid arthritis. *Nat Genet.* 2003;35:341-8.
8. Peltekova VD, Wintle RF, Rubin LA, Amos CI, Huang Q, Gu X, et al. Functional variants of OCTN cation transporter genes are associated with Crohn disease. *Nat Genet.* 2004;36:471-5.
9. Yamazaki K, Takazoe M, Tanaka T, Ichimori T, Saito S, Iida A, et al. Association analysis of *SLC22A4*, *SLC22A5* and *DLG5* in Japanese patients with Crohn disease. *J Hum Genet.* 2004;49:664-8.
10. Fisher SA, Hampe J, Onnie CM, Daly MJ, Curley C, Purcell S, et al. Direct or indirect association in a complex disease: the role of *SLC22A4* and *SLC22A5* functional variants in Crohn disease. *Hum Mutat.* 2006;27:778-85.
11. Shekhawat PS, Srinivas SR, Matern D, Bennett MJ, Boriack R, George V, et al. Spontaneous development of intestinal and colonic atrophy and inflammation in the carnitine-deficient *jvs* (*OCTN2*^(-/-)) mice. *Mol Genet Metab.* 2007;92:315-24.

12. Asano M, Furukawa K, Kido M, Matsumoto S, Umesaki Y, Kochibe N, et al. Growth retardation and early death of beta-1,4-galactosyltransferase knockout mice with augmented proliferation and abnormal differentiation of epithelial cells. *EMBO J.* 1997;16:1850-7.
13. Soriano P, Montgomery C, Geske R, Bradley A. Targeted disruption of the c-src proto-oncogene leads to osteoporosis in mice. *Cell.* 1991;64:693-702.
14. Yagi T, Nada S, Watanabe N, Tamemoto H, Kohmura N, Ikawa Y, et al. A novel negative selection for homologous recombination using diphtheria toxin A fragment gene. *Anal Biochem.* 1993;214:77-86
15. Tamai I, Ohashi R, Nezu JI, Sai Y, Kobayashi D, Oku A, et al. Molecular and functional characterization of organic cation/carnitine transporter family in mice. *J Biol Chem.* 2000;275:40064-72.
16. Soga T, Baran R, Suematsu M, Ueno Y, Ikeda S, Sakurakawa T, et al. Differential metabolomics reveals ophthalmic acid as an oxidative stress biomarker indicating hepatic glutathione consumption. *J Biol Chem.* 2006;281:16768-76.
17. Soga T, Ishikawa T, Igarashi S, Sugawara K, Kakazu Y, Tomita M. Analysis of nucleotides by pressure-assisted capillary electrophoresis mass spectrometry using silanol mask technique. *J Chromatogr A.* 2007;1159:125-33.

18. Malathi P, Preiser H, Fairclough P, Mallett P, Crane RK. A rapid method for the isolation of kidney brush border membranes. *Biochim Biophys Acta*. 1979;554:259-63.
19. Nakamura T, Yoshida K, Yabuuchi H, Maeda T, Tamai I. Functional characterization of ergothioneine transport by rat organic cation/carnitine transporter Octn1 (slc22a4). *Biol Pharm Bull*. 2008;31:1580-4.
20. Brummel MC. In search of a physiological function for L-ergothioneine-II. *Med Hypotheses*. 1989;30:39-48.
21. Fahey RC. 2001. Novel thiols of prokaryotes. *Annu Rev Microbiol*. 2001;55:333-56.
22. Tamai I, Nakanishi T, Kobayashi D, China K, Kosugi Y, Nezu J, et al. Involvement of OCTN1 (SLC22A4) in pH-dependent transport of organic cations. *Mol Pharm*. 2004;1:57-66.
23. Chaudière J, Ferrari-Iliou R. Intracellular antioxidants: from chemical to biochemical mechanisms. *Food Chem Toxicol*. 1999;37:949-62.
24. Sakrak O, Kerem M, Bedirli A, Pasaoglu H, Akyurek N, Ofluoglu E, et al. Ergothioneine modulates proinflammatory cytokines and heat shock protein 70 in mesenteric ischemia and reperfusion injury. *J Surg Res*. 2008;144:36-42.
25. Nikolaus S, Schreiber S. Diagnostics of inflammatory bowel disease. *Gastroenterology*. 2007;133:1670–89.

26. Kobayashi D, Aizawa S, Maeda T, Tsuboi I, Yabuuchi H, Nezu J, et al. Expression of organic cation transporter OCTN1 in hematopoietic cells during erythroid differentiation. *Exp Hematol*. 2004; 32:1156-62.
27. Wijnholds J, Evers R, van Leusden MR, Mol CA, Zaman GJ, Mayer U, et al. Increased sensitivity to anticancer drugs and decreased inflammatory response in mice lacking the multidrug resistance-associated protein. *Nat Med*. 1997;11:1275-9.
28. Jonker JW, Wagenaar E, Van Eijl S, Schinkel AH. Deficiency in the organic cation transporters 1 and 2 (Oct1/Oct2 [Slc22a1/Slc22a2]) in mice abolishes renal secretion of organic cations. *Mol Cell Biol*. 2003;21:7902-8.
29. Kawano H, Otani M, Takeyama K, Kawai Y, Mayumi T, Hama T. Studies on ergothioneine. VI. Distribution and fluctuations of ergothioneine in rats. *Chem Pharm Bull*. 1982;30:1760-5.
30. Melville DB, Horner WH, Otken CC, Ludwig ML. Studies of the origin of L-Ergo in animals. *J Biol Chem*. 1955;213:61-8.

Legends to Figures

Fig. 1. Metabolome analysis revealed almost complete loss of ergothioneine in *octn1*^{-/-} mice

The data shown represent the heat map indicating overall difference in the amount of 112 metabolites in each tissue and erythrocytes between wild-type and *octn1*^{-/-} mice. Each column in the abscissa represents expression index which scales relative amount of the metabolite in each tissue and erythrocytes of wild-type mice to that in *octn1*^{-/-} mice (N = 3 for each strain). Each column in the ordinate represents each metabolite, and the arrowhead indicates ergothioneine.

Fig. 2. Uptake of [³H]ergothioneine by mouse OCTN1

(A) Time course of [³H]ergothioneine uptake by mouse OCTN1. HEK293 cells were transiently transfected with OCTN1 (open circles), OCTN2 (open triangles) or vector alone (closed circles), and uptake of [³H]ergothioneine (3.4 μM) was then measured over 10 min at pH 7.4. The uptake was expressed as cell-to-medium ratio, which was obtained by dividing the amount taken up in the cells by substrate concentration in the medium. Each value represents the mean ± SEM (n = 3). When error bars are not shown, they are smaller than the symbols.

(B) Concentration dependence of [^3H]ergothioneine uptake by mouse OCTN1. Uptake of various concentrations of [^3H]ergothioneine was measured over 5 min at pH 7.4. The closed and open circles represent the uptake by HEK293 cells expressing OCTN1 and vector alone, respectively. Each line was obtained by nonlinear least-squares analysis. A solid line represents the OCTN1-mediated uptake after subtraction of the uptake by mock cells from that by OCTN1-expressing cells.

(C) Sodium dependence of [^3H]ergothioneine uptake by mouse OCTN1. Uptake of [^3H]ergothioneine was measured over 5 min at pH 7.4 in the presence (closed columns) or absence (open columns) of Na^+ . In the absence of Na^+ , Na^+ was replaced with N-methyl-D-glucamine.

Fig. 3. Absorption and disposition of [^3H]ergothioneine after oral administration.

[^3H]Ergothioneine was orally administered in wild-type (open circles) and *octn1*^{-/-} (closed circles) mice, and plasma (A) and blood (B) concentrations, and cumulative urinary excretion (C) were determined for 14 days. Each value represents the mean \pm SEM (n = 3 - 6).

Fig. 4. Ergothioneine is highly distributed to small intestine after oral administration

[^3H]Ergothioneine remaining in plasma and tissues was determined 4 hrs (A) and 14 days (B) after oral administration in wild-type (open bars) and *octn1*^{-/-} (closed bars) mice. The data showing the

tissue-to-plasma concentration ratio less than 10 were enlarged in the inset of panel A. Each value represents the concentration ratio between the indicated tissue and plasma, and is shown as mean \pm SEM (n = 3 - 4).

*, Significantly different from wild-type mice by Student's t test ($p < 0.05$).

Fig. 5. Ergothioneine protects small intestine from lethal injury.

(A) Survival curves of wild-type (n=6, open) or *octnI*^{-/-} mice (n=7, closed) after ischemia (60 min) and reperfusion. $P < 0.05$ (log-rank test).

(B) Histology of the intestinal mucosa. Wild-type (left) and *octnI*^{-/-} (right) mice were subjected to gut ischemia-reperfusion. At 30 min after reperfusion, the intestine was removed and stained with H&E.

Original magnification, x 200

Fig. 6. Ergothioneine concentration in blood of healthy volunteers (n = 31), patients with CD (n = 25) and those with UC (n = 16)

The horizontal lines and squares within each box represent the median and the arithmetic mean, respectively. The box edges show the lower (25th) and upper (75th) quartiles. The whiskers extend from the 25th and 75th quartiles to the furthest data points within a distance of 1.5 interquartile ranges

from the 25th and 75th quartiles. Circles outside whiskers represent outliers. Statistical comparisons were performed using one-way ANOVA with Dannett's multiple comparison test.*, Significantly different from healthy volunteers ($p < 0.001$)

Figure 1

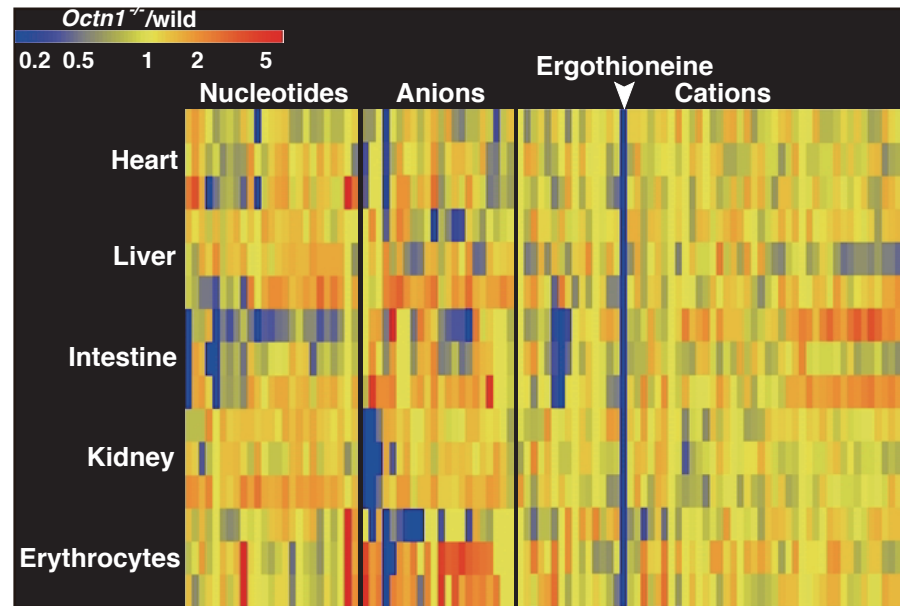


Table I. Tissue concentration of ergothioneine in wild-type and *octn1*^{-/-} mice^{a)}

	Ergothioneine Concentration ($\mu\text{g/g}$ tissue or mL)			
	Wild-type			<i>octn1</i> ^{-/-}
Intestine (Upper)	13.7	±	2.6	< 1.07
Intestine (Middle)	22.2	±	1.3	< 2.13
Intestine (Lower)	14.2	±	2.5	< 2.13
Large Intestine	3.32	±	0.59	< 1.07
Liver	121	±	25	< 2.13
Pancreas	6.02	±	0.20	< 2.13
Kidney	35.9	±	2.8	< 2.13
Spleen	17.8	±	1.8	< 2.13
Heart	26.9	±	6.2	< 2.13
Lung	17.4	±	3.0	< 2.13
Thymus	5.32	±	0.90	< 1.07
Muscle	3.58	±	0.12	< 1.07
Testis	4.76	±	0.51	< 1.07
Brain	1.45	±	0.30	< 1.07
Skin	19.2	±	2.3	< 1.07
Blood	16.5	±	0.6	< 2.13
Erythrocytes	22.1	±	1.2	< 1.07
Plasma	0.179	±	0.024	< 0.15
Urine		< 2.13		< 1.07

^{a)} Concentration of ergothioneine was measured by HPLC

Figure 2

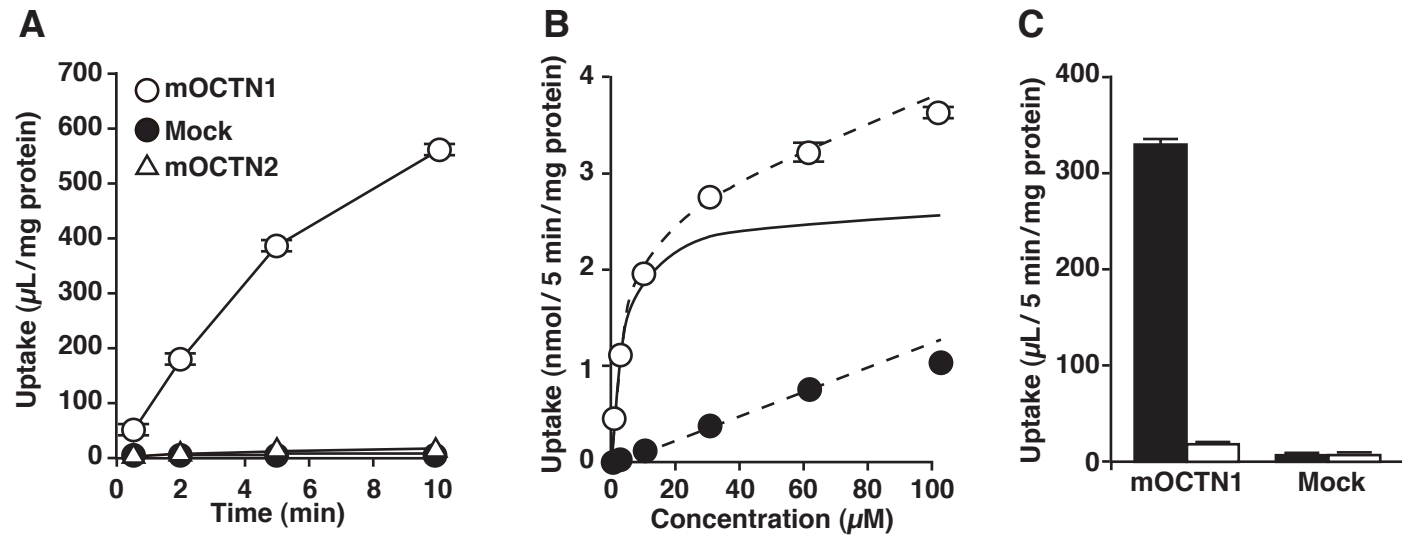


Figure 3

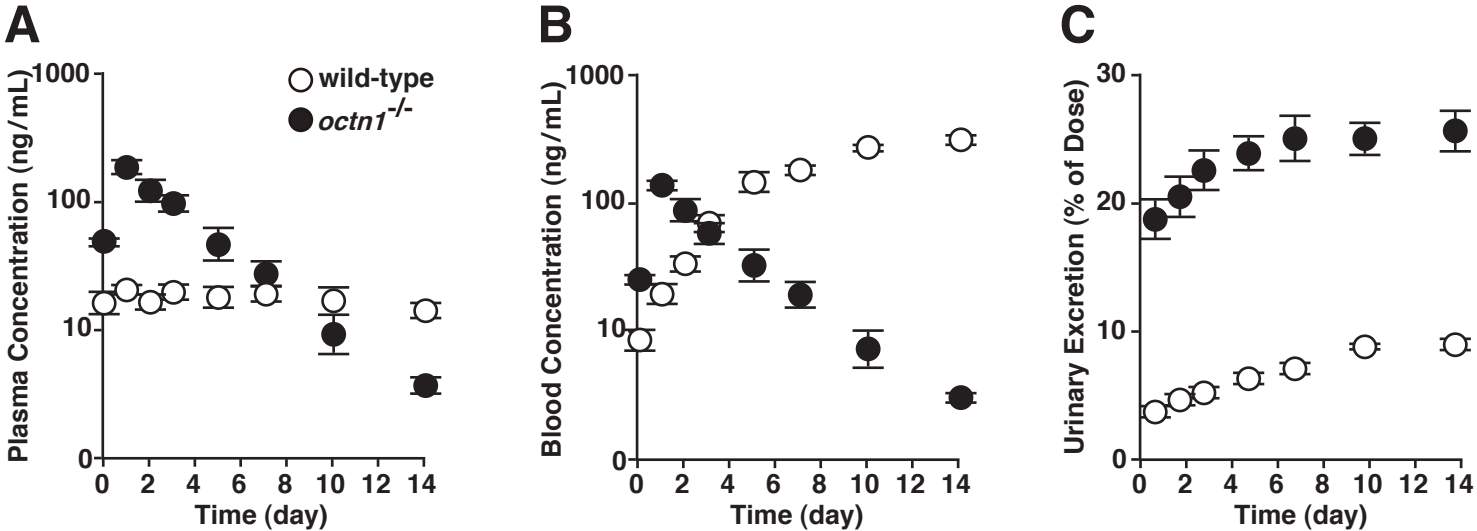


Figure 4 A

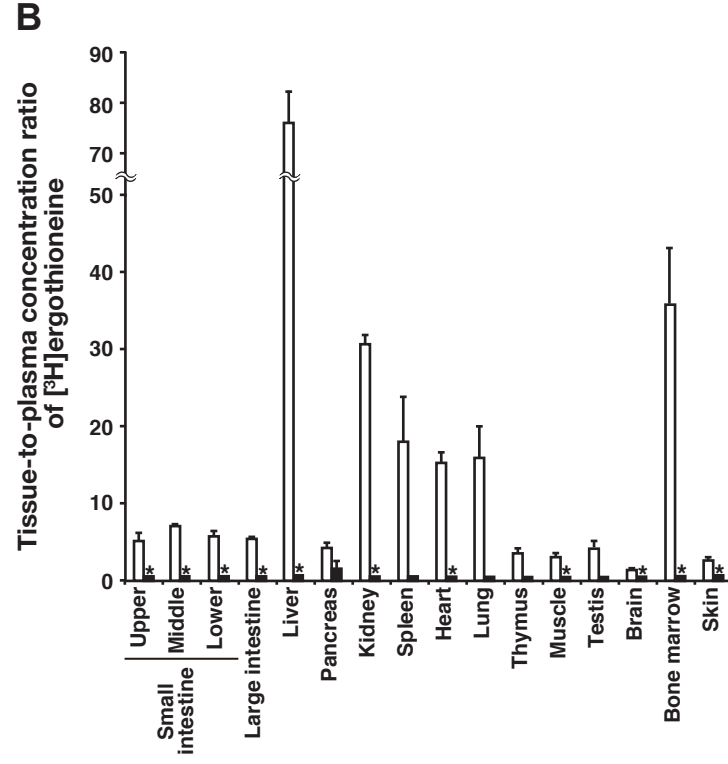
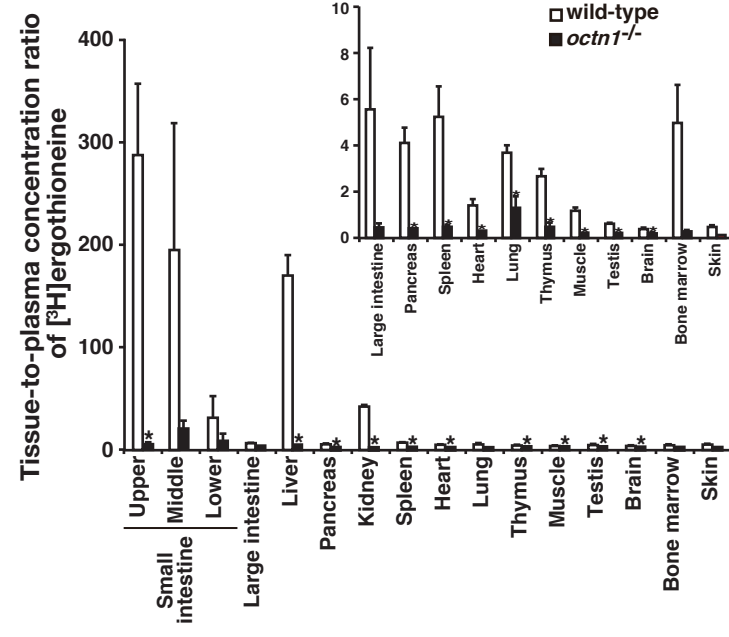


Figure 5

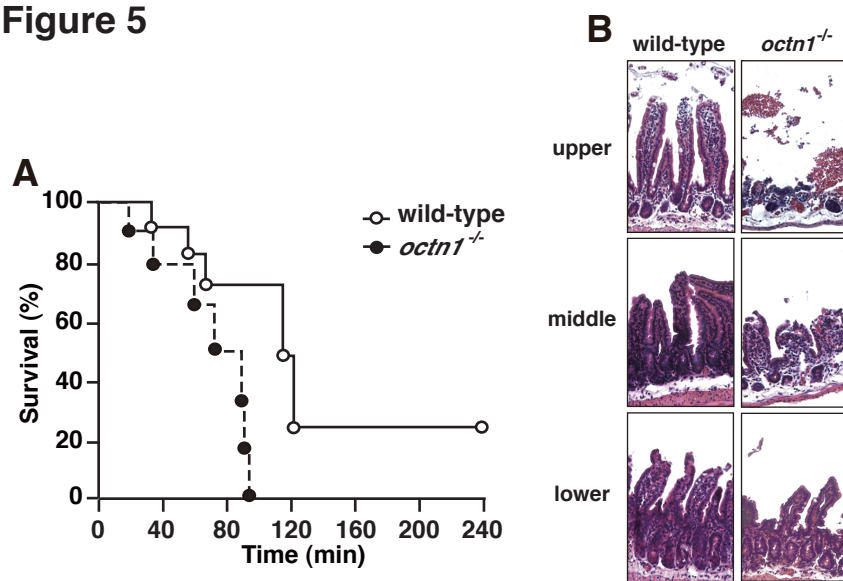
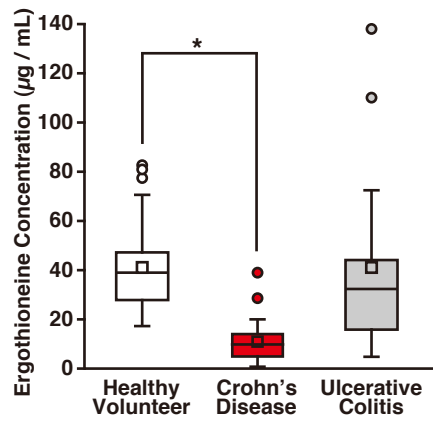


Figure 6



Supplemental Table 1. List of Primers for Genotyping in Human

Genes	Amplified and sequenced regions	Forward primers		Reverse primers		PCR products (bp)	Annealing temperature (°C)	Extension time (s)
		Sequences (5' to 3')	Positions* ¹	Sequences (5' to 3')	Positions* ¹			
<i>SLC22A4 /OCTN1</i>	exon_1	AAGCCCCGTCAGGTCCTTG	34044971	TTTCTTGGGGTGCACACCCG	34045871	901	62	60
	exon_2	CAGTCAAACCCAGGGCTGCAAGGCCTATG	34062700	GTCCAGCCCCAAGATAGGCAGTGATTGAC	34063039	341	68	25
	exon_3	CATTGATGCCTGACTCAGGGCTTGCAACAC	34064241	ACTTGCTCCAAGAGCTGTGGCTACGGCTCC	34064626	386	68	25
	exon_4	CAAGTCTTGGATCACGTCCCAC	34072711	AGGCTAGGTCAGCATCAGGC	34073162	452	62	40
	exon_5	CAAGCACAACCTGATGATCGGTC	34077765	TGATTGTGTTCCCTAAGGCCTAGTGC	34078241	477	60	35
	exon_6	CATGCATAAGTTTTCCCCATGCATCATAGC	34082374	GAAAACCCAGTCGTTGTCATAATGTTCCCTC	34082655	282	64	30
	exon_7	CAATGAGGGTAGTGGCTACTTATAAGACAG	34085311	TGATGTAAAGGCTGAATAAACATGGAGCAGTG	34085739	429	64	35
	exon_8	AAAAGTACTCCCACTGAAGC	34086425	CAAAATGTCTGTAGCGCTACTC	34086893	469	56	40
	exon_9	CCAACCTCACAAAATGATGCTCAAGAGTGCCC	34091192	CTATTTCAGAACCTTCCTAGCTATTCTTCC	34091491	300	60	25
	exon_10	ATCTACACCATGAGGTTCTCATTAGAGTTC	34094321	GAGTGTGGAAGGTTTTCTGGATAGGAATAC	34095037	717	62	50
<i>SLC22A5 /OCTN2</i>	5'UTR	AGTCCCGCTGCCTTCCTAAG	34120255	GTCACCTCGTCGTAGTCCCG	34120700	446	58	40
	exon_1	GCAGGACCAAGGCGGCGGTGTCAG	34120513	AGCTCGGGTTCAAGGACCGC	34121141	629	63	45
	exon_2	CCTGACTAAGTGAGTTCACA	34128953	TCAAGGGCCAGGCACACGCT	34129257	305	58	25
	exon_3	TGTGAGACCGAGACTGTCCCTG	34134702	CCCTGCCTGTAAGTAAGGTTCA	34135141	440	58	40
	exon_4	GGAACCCAAATTAACCTGC	34135988	CTGCCCTCTAGTGAAGGCCA	34136275	288	51	25
	exon_5	GGTTCTGCAACCTTATTC	34137631	AGGGCTGGGTGCTGCTGCTC	34137927	297	51	25
	exon_6	TCTGACCACCTCTTCTCCCATAC	34139581	TAAAACAAGAGGCCCAATGGC	34139797	217	58	25
	exon_7	TACAGGTTGGGAAAGATG	34141337	ATTGAGACAGCCTGGTAGAC	34141680	344	53	25
	exon_8	TATGTTTGTGTTGCTCTCAATAGC	34143063	CAGCTCAAACATTCAAGCCAGT	34143391	329	56	25
	exon_9	AGAGTCCTGGGAGCATAA	34144298	TCTGTGAGAGGGAGTTTGCGAGTA	34144605	308	60	25
exon_10	CTTGTTTGTGTTGGAGACTG	34144820	CTGCACAAGCTGGCCATTC	34145046	227	53	25	

*1, Nucleotide positions of the 5' end of each primer in NT_034772.5

Supplemental Table 2. Biochemical parameters of sera from wild-type and *octn1*^{-/-} mice in 8 weeks old

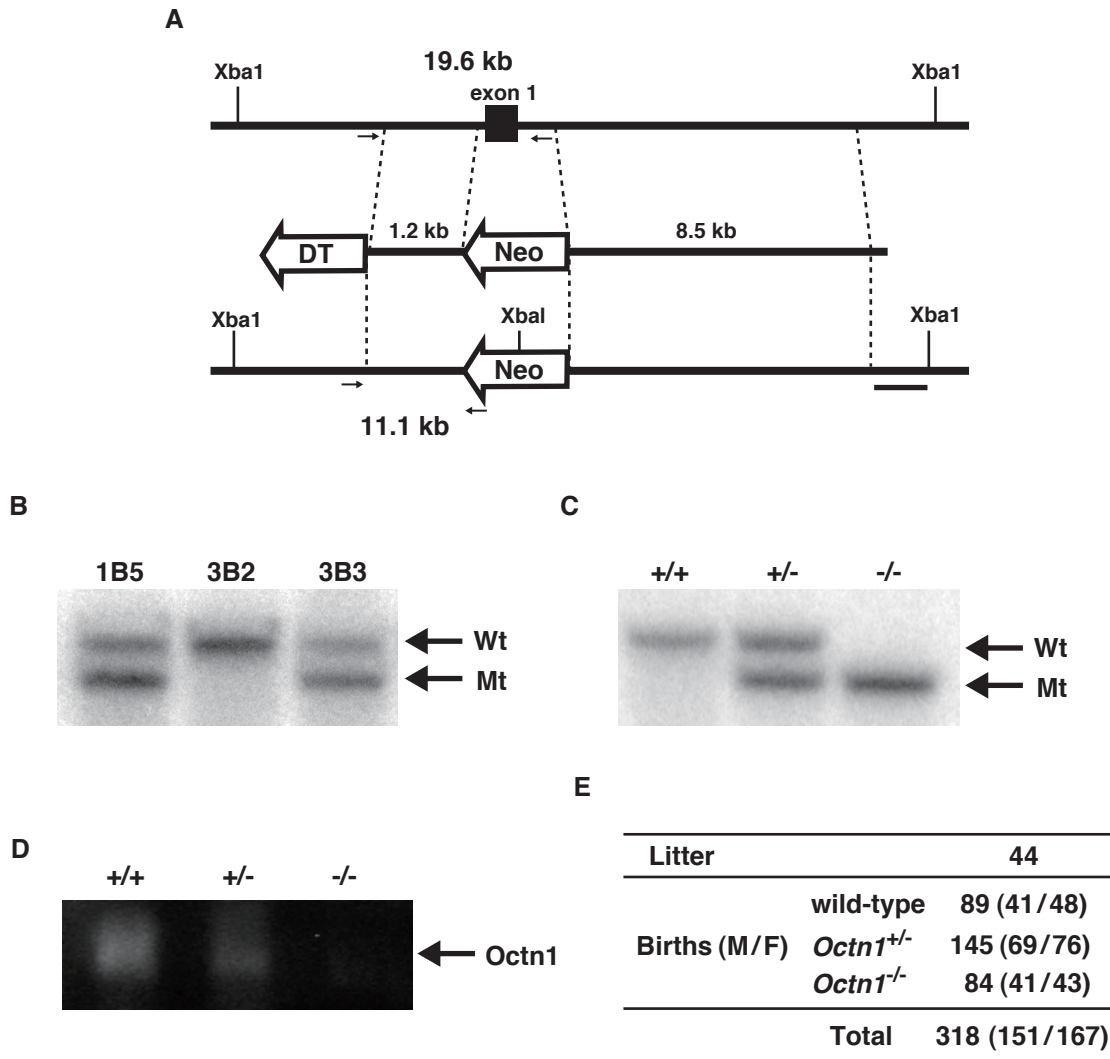
		Male						Female					
		Wild-type			<i>Octn1</i> ^{-/-}			Wild-type			<i>Octn1</i> ^{-/-}		
Total protein	g/dL	4.35	±	0.03	4.33	±	0.06	4.24	±	0.13	4.18	±	0.10
Albumin	g/dL	2.23	±	0.10	2.23	±	0.08	2.34	±	0.07	2.35	±	0.07
A/G		1.08	±	0.08	1.08	±	0.05	1.24	±	0.02	1.3	±	0.04
CK	IU/L	280	±	89	168	±	34	135	±	11	123	±	11
AST(GOT)	IU/L	62.5	±	7.4	59.5	±	5.2	61.4	±	2.7	51.3	±	1.1*
ALT(GPT)	IU/L	28	±	3.3	30.8	±	8.0	19.2	±	1.2	17.5	±	1.2
LDH	IU/L	526	±	128	396	±	48	391	±	28	299	±	25*
ALP	IU/L	315	±	24	299	±	20	479	±	12	466	±	43
γ -GTP	IU/L	1	±	0	1	±	0	1	±	0	1	±	0
Creatinine	Mg/dL	0.11	±	0.01	0.1	±	0.01	0.114	±	0.002	0.09	±	0.004*
Urinary acid	Mg/dL	1.93	±	0.19	1.85	±	0.03	1.4	±	0.2	1.25	±	0.25
Urea nitrogen	Mg/dL	30	±	1.5	27.3	±	2.6	27.2	±	1.5	27	±	1.41
Sialic acid	Mg/dL	28.3	±	2.0	29.8	±	1.0	16.6	±	0.2	17.8	±	0.5
Total lipid	Mg/dL	415	±	32	474	±	27	332	±	16	313	±	12
TG	Mg/dL	61.3	±	13.5	92.3	±	24.2	40.6	±	7.1	45.8	±	5.2
Phospholipid	Mg/dL	208	±	14	221	±	7	166	±	9	155	±	5
Free fatty acid	mEq/L	1.14	±	0.07	1.29	±	0.13	1.27	±	0.12	1.29	±	0.17
Total cholesterol	Mg/dL	97	±	6.5	107	±	6	83.6	±	4.8	74.5	±	3.8
Total bile acids	μmol/L	3.53	±	0.89	7.65	±	5.96	12.8	±	8.7	9.38	±	6.53
Cl	mEq/L	113	±	1	113	±	1	114	±	1.0	113	±	1
Ca	Mg/dL	8.98	±	0.11	9	±	0.04	8.74	±	0.09	8.78	±	0.11
Total bilirubin	Mg/dL	0.1	±	0	0.1	±	0	0.1	±	0	0.1	±	0
Direct bilirubin	Mg/dL	0	±	0	0	±	0	0	±	0	0	±	0
Indirect bilirubin	Mg/dL	0.1	±	0	0.1	±	0	0.1	±	0	0.1	±	0
CRP	Mg/dL	0.0075	±	0.003	0.0075	±	0.003	0.002	±	0.002	0.005	±	0.003

Mean ± S.E.M, *p< 0.05

Supplemental Table 3. Allele Frequency of SLC22A4/OCTN1 and SLC22A5/OCTN2

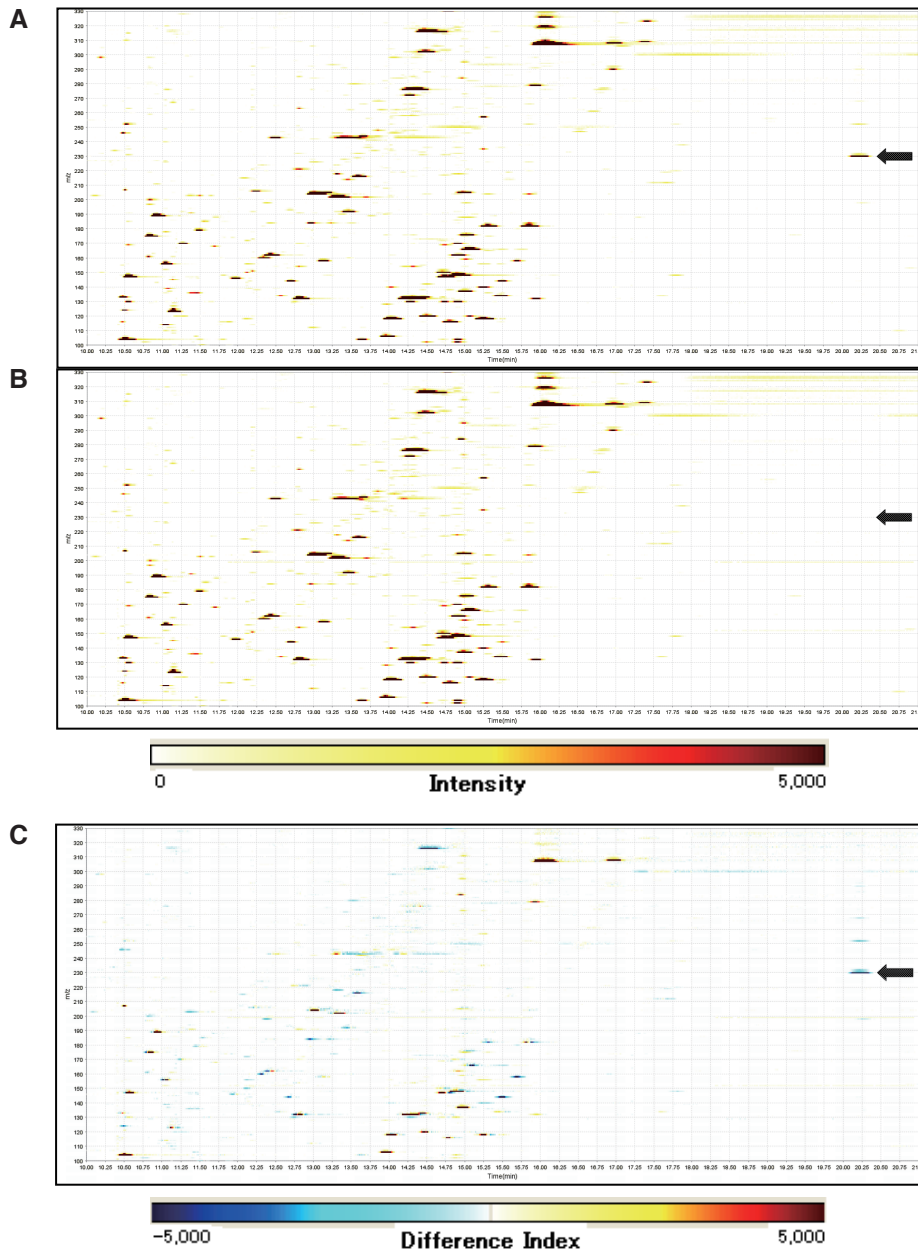
Gene	Region	SNP ^{*1}	Allele		Genotype								Allele1 versus Allele2		
			1	2	CD			Control			Odds ratio (95% c.i.)	χ^2	P value		
					11	12	22	sum	11	12				22	sum
<i>SLC22A4</i> <i>/OCTN1</i>	5'UTR	rs460271	G	C	0	6	4	10	1	4	5	10	1.00 (0.26-3.87)	0.00	1.000
		L148V	C	G	256	0	0	256	19	0	0	19	-	-	-
	exon_2	L155L	C	T	256	0	0	256	19	0	0	19	-	-	-
		V159M	G	A	256	0	0	256	19	0	0	19	-	-	-
		D165G	A	G	256	0	0	256	19	0	0	19	-	-	-
		Q180H	G	C	37	0	0	37	19	0	0	19	-	-	-
		F185F	C	T	37	0	0	37	19	0	0	19	-	-	-
	exon_3	I202I	C	T	37	0	0	37	19	0	0	19	-	-	-
		M205I	G	A	37	0	0	37	19	0	0	19	-	-	-
		rs3761659 ^{*1}	G	C	5	4	1	10	21	19	5	45	1.11 (0.39-3.18)	0.04	0.847
	intron_4	rs270600 ^{*1}	T	C	0	0	10	10	0	1	44	45	-	0.22	0.636
	exon_5	R282stop	C	T	43	0	0	43	19	0	0	19	-	-	-
		I306T	T	C	70	68	20	158	32	39	5	76	0.85 (0.58-1.25)	0.69	0.406
	intron_6	rs2304081 ^{*1}	G	A	4	5	1	10	21	14	10	45	1.13 (0.41-3.10)	0.05	0.816
	exon_7	T394T	C	G	125	103	28	256	32	39	5	76	1.00 (0.69-1.43)	0.00	0.985
		V411V ^{*1}	G	C	256	0	0	256	19	0	0	19	-	-	-
	exon_8	G462E	G	A	43	0	0	43	19	0	0	19	-	-	-
		G471G	C	G	43	0	0	43	19	0	0	19	-	-	-
	exon_9	L503F	C	T	256	0	0	256	19	0	0	19	-	-	-
<i>SLC22A5</i> <i>/OCTN2</i>	5'UTR	-207G→C	G	C	78	0	0	78	76	0	0	76	-	-	-
		rs13180169	G	T	36	35	7	78	20	48	8	76	1.59 (1.00-2.53)	3.79	0.052
		rs13180186	G	T	34	37	7	78	20	48	8	76	1.50 (0.94-2.38)	2.92	0.088
	exon_1	rs13180043	C	T	35	36	7	78	20	48	8	76	1.54 (0.97-2.46)	3.34	0.068
		rs13180295	G	A	37	34	7	78	20	48	8	76	1.64 (1.02-2.61)	4.28	0.039
		L95L	T	C	13	28	37	78	4	38	34	76	1.22 (0.76-1.97)	0.67	0.415
	exon_2	L114P	T	C	78	0	0	78	76	0	0	76	-	-	-
		L144F ^{*1}	C	T	10	0	0	10	44	0	0	44	-	-	-
	exon_3	F189L ^{*1}	T	C	10	0	0	10	43	0	0	43	-	-	-
	exon_4	L269L	A	G	12	28	38	78	4	36	36	76	1.23 (0.76-1.99)	0.69	0.406
	intron_4	rs274557	T	C	12	28	38	78	4	36	36	76	1.23 (0.76-1.10)	0.69	0.406
	exon_6	Q326Q ^{*1}	G	A	10	0	0	10	-	-	-	-	-	-	-
		Y449D ^{*1}	T	G	10	0	0	10	43	0	0	43	-	-	-
		V481F	G	T	10	0	0	10	-	-	-	-	-	-	-
	exon_8	V481I	G	A	10	0	0	10	-	-	-	-	-	-	-
		G484V	G	T	10	0	0	10	-	-	-	-	-	-	-
		R488H	G	A	10	0	0	10	-	-	-	-	-	-	-
	exon_9	F508F	T	C	10	0	0	10	-	-	-	-	-	-	-
		Q523R	A	G	10	0	0	10	-	-	-	-	-	-	-
exon_10	M530V	A	G	10	0	0	10	-	-	-	-	-	-	-	

*1, Genotype in control was cited from the data obtained in HapMap project for Japanese population in Tokyo.



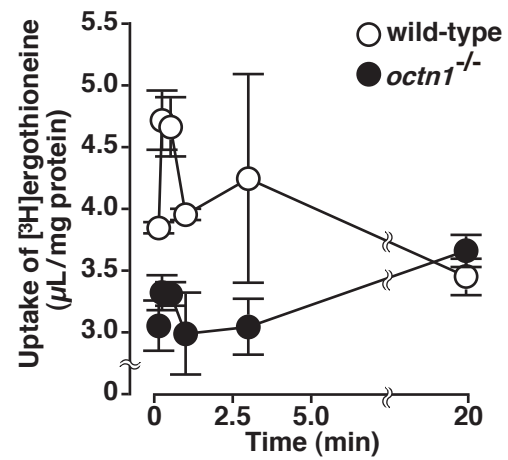
Generation of *octn1*^{-/-} mice (A) Targeted disruption of the *slc22a4/octn1* gene by homologous recombination. The PGKneobpA cassette (Neo) and the DT-A cassette (DT-A) are indicated with white arrows. Exon 1 of the *octn1* gene, which includes the start codon, is shown as a closed box. PCR primers used for screening are shown as arrows. The black bars show the positions of external probes used for Southern blot analysis. **(B)** Southern blot analysis of ES cell clones. Genomic DNA (10 μ g) from ES cell clones (1B5, 3B2, 3B3) was digested with Xba I and hybridized with the probe. The expected DNA fragments for the mutant (Mt) and wild-type (Wt) alleles are indicated (11.1 and 19.6 kb, respectively). **(C)** Southern blot analysis of wild-type and *octn1*^{-/-} mice. Genomic DNA (10 μ g) from liver was digested with Xba I and hybridized with the probe. The expected DNA fragments for the mutant and wild-type alleles are indicated. **(D)** Western blot analysis of wild-type and *octn1*^{-/-} mice. The lysates of membrane fraction obtained from kidneys were loaded onto SDS-PAGE. Slc22a4/Octn1 protein was detected with a rabbit anti-Octn1 antibody. A band (arrow), which corresponds to the molecular mass of Octn1 (70 kD), was detected in wild-type and *octn1*^{+/-} mice. **(E)** Birthrate of wild-type and *octn1*^{-/-} mice.

Supplemental Figure 2



Metabolomic analysis in *octn1*^{-/-} mice. The data shown represent a typical result for detection of cationic metabolites in erythrocytes of wild-type (A) and *octn1*^{-/-} (B) mice. In panel (C), metabolome differential displays are shown, and the gradation of the color bar indicates increase (red) or decrease (blue) of the metabolite level in *octn1*^{-/-} mice. Ergothioneine in each panel was indicated with arrows.

Supplemental Figure 3



Time course of [³H]ergothioneine uptake by brush border membrane vesicles (BBMVs) of wild-type and *octn1*^{-/-} mice. Membrane vesicles were suspended in the buffer (pH 7.4). Uptake of [³H]ergothioneine (3.4 µM) by BBMVs of wild-type (open circles) and *octn1*^{-/-} (closed circles) mice were measured at 25 ° C in the uptake buffer at pH 7.4. Data were expressed as vesicle-to-medium ratio, which was obtained by dividing the amount taken up in the vesicles by substrate concentration in the uptake medium. Each result represents the mean ± S. E. M. (n = 3).